Observation of High-Order Polarization-Locked Vector Solitons in a Fiber Laser

D. Y. Tang, H. Zhang, L. M. Zhao, and X. Wu

School of Electrical and Electronic Engineering, Nanyang Technological University, Singapore 639798

(Received 13 March 2008; revised manuscript received 30 August 2008; published 10 October 2008)

We report on the experimental observation of a new type of polarization-locked vector soliton in a passively mode-locked fiber laser. The vector soliton is characterized by the fact that not only are the two orthogonally polarized soliton components phase-locked, but also one of the components has a double-humped intensity profile. Multiple phase-locked high-order vector solitons with identical soliton parameters and harmonic mode locking of the vector solitons were also obtained in the laser. Numerical simulations confirmed the existence of stable high-order vector solitons in the fiber laser.

DOI: 10.1103/PhysRevLett.101.153904 PACS numbers: 42.81.Dp, 05.45.Yv

Solitons, as stable localized nonlinear waves, have been observed in various physical systems and have been extensively studied [1,2]. Optical solitons were first experimentally observed in single mode fibers (SMFs) by Mollenauer, Stolen, and Gordon in 1980 [3]. It was shown that the dynamics of the solitons could be well described by the nonlinear Schrödinger equation, a paradigm equation governing optical pulse propagation in ideal SMFs. However, in reality, a SMF always supports two orthogonal polarization modes. Taking fiber birefringence into account, it was later found that, depending on the strength of fiber birefringence, different types of vector solitons, such as the group velocity-locked vector solitons [4,5], the rotating polarization vector solitons [6,7], and the phase-locked vector solitons [8–10], could also be formed in SMFs.

Optical solitons were also observed in mode-locked fiber lasers. Pulse propagation in a fiber laser cavity is different from that in a SMF. Apart from propagating in the fibers that form the laser cavity, a pulse propagating in a laser is also subject to actions of the laser gain and other cavity components. The dynamics of solitons formed in a fiber laser are governed by the Ginzburg-Landau (GL) equation, which takes account not only of the fiber dispersion and Kerr nonlinearity but also the laser gain and losses. However, it was shown that, under suitable conditions, solitons formed in fiber lasers have analogous features to those of solitons formed in SMFs. Furthermore, vector solitons were also predicted in mode-locked fiber lasers and recently confirmed experimentally [11,12].

Among the various vector solitons formed in mode-locked fiber lasers or SMFs, the phase-locked one has attracted considerable attention. Back in 1988, Christodoulides and Joseph first theoretically predicted a form of phase-locked vector soliton in birefringent dispersive media [8], which is now known as a high-order phase-locked vector soliton in SMFs. The fundamental form of the phase-locked vector solitons was recently experimentally observed [12–14]. However, to the best of our knowledge, no high-order temporal vector solitons have been demonstrated. Numerical studies have shown that the high-order phase-locked vector solitons are unstable in SMFs [7]. In this Letter, we report on the experimental observation of a stable phase-locked high-order vector soliton in a mode-locked fiber laser. Multiple high-order vector solitons with identical soliton parameters coexisting in a laser cavity and harmonic mode locking of the high-order vector solitons were also observed. Moreover, based on a coupled Ginzburg-Landau equation model, we show numerically that phase-locked high-order vector solitons are stable in mode-locked fiber lasers.

The experimental setup is shown in Fig. 1. The fiber laser has a ring cavity consisting of a 4.6 m length of erbium-doped fiber with group velocity dispersion parameter 10 ps/km/nm and a total length of 5.4 m of standard SMF with group velocity dispersion parameter 18 ps/km/nm. Mode locking of the laser is achieved with a semiconductor saturable absorption mirror (SESAM). A polarization-independent circulator was used to force the unidirectional operation of the ring and simultaneously to incorporate the SESAM in the cavity.

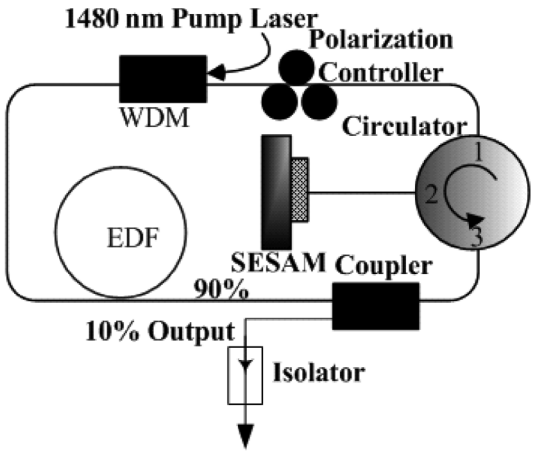

FIG. 1. Schematic of the vector soliton fiber laser. WDM: Wavelength division multiplexer. EDF: Erbium-doped fiber.

Note that within one cavity round-trip the pulse propagates twice in the SMF between the circulator and the SESAM. The laser was pumped by a high power fiber Raman laser source (BWC-FL-1480-1) of wavelength 1480 nm. A 10% fiber coupler was used to output the signals. The SESAM used was based on GaInNAs quantum wells. It has a saturable absorption modulation depth of 5%, a saturation fluence of 90 $\mu J/cm^2$, and a recovery time of 10 ps. The central absorption wavelength of the SESAM is at 1550 nm. A fiber polarization controller was inserted in the cavity to fine-tune the net cavity birefringence.

As no polarizer was used in the cavity, depending on the net cavity linear birefringence, various types of vector solitons such as the group velocity-locked vector soliton, the polarization rotating vector soliton, and the fundamental phase-locked vector soliton were obtained in the laser. We found that the experimentally observed features of these vector solitons could be well described by an extended coupled Ginzburg-Landau equation model, which also considered the effects of the saturable absorber and the laser cavity [15]. Encouraged by the results, we then further searched for the high-order phase-locked vector solitons theoretically predicted. Through splicing a fiber-pigtailed optical isolator between the output port and the external cavity measurement apparatus, which serves to suppress the influence of backreflections on the operation of the laser, we could indeed obtain one such vector soliton. Figure 2 shows, for example, the optical spectra and autocorrelation traces of the soliton observed. Polarization locking of the soliton is identified by measuring the polarization evolution frequency (PEF) of the soliton pulse train [13,14]. No PEF could be detected. As the vector soliton has a stationary elliptic polarization, we could use an external polarizer to separate its two orthogonal polarization components. The optical spectra of the components are shown in Fig. 2(a). The spectra have the same central wavelength and about 10 dB peak intensity difference. Both spectra display soliton sidebands, showing that both of the components are solitonic. In addition, coherent energy exchange between the two soliton components, represented by the appearance of spectral peak-dip sidebands [15], is also visible in the spectra. However, in contrast to the polarization resolved spectra of the fundamental phase-locked vector solitons, there is a strong spectral dip at the center of the spectrum of the weaker component. No such dip appears in the spectrum of the stronger component. To identify the cause of the spectral dip, we further measured the autocorrelation traces of each of the soliton components. It turned out that the weak component of the vector soliton had a double-humped intensity profile as shown in Fig. 2(b). The pulse width of the humps is about 719 fs if a $sech^2$ profile is assumed, and the separation between the humps is about 1.5 ps. The strong component of the vector soliton is a single-hump soliton. It has a pulse width of about 1088 fs if a $sech^2$

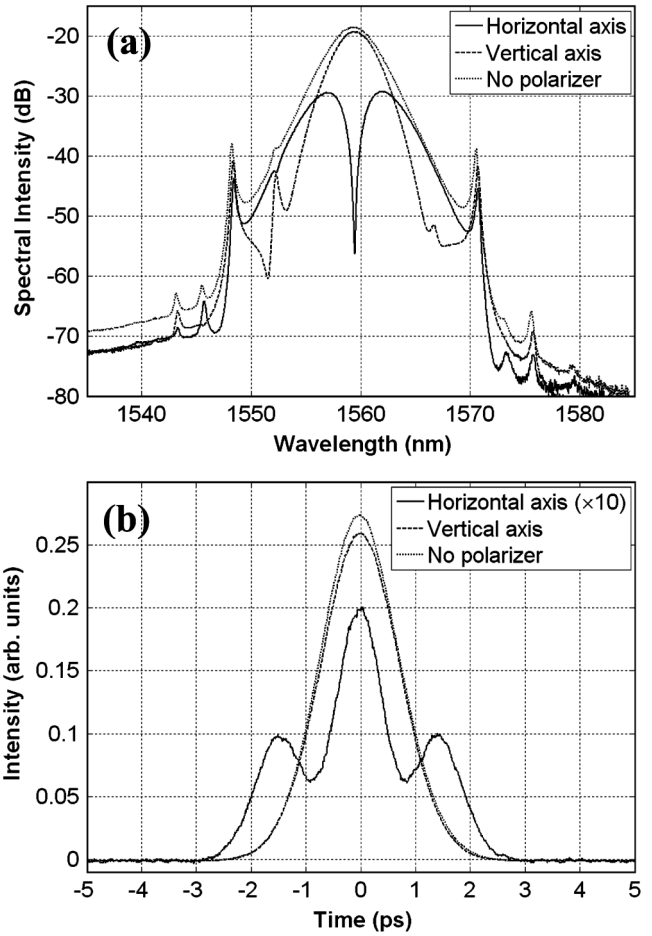

FIG. 2. Polarization resolved soliton spectra and autocorrelation traces of the vector soliton observed. (a) Soliton spectra. (b) Autocorrelation traces.

profile is assumed. The components of the vector soliton have pulse intensity profiles exactly like those predicted by Akhmediev *et al.* [10] and Christodoulides [8] for a high-order phase-locked vector soliton. Based on the autocorrelation traces, obviously the spectral dip is formed due to the spectral interference between the two humps, and the strong dip at the center of the spectrum indicates that the two humps have 180° phase difference, which is also in agreement with the theoretical prediction.

Once the laser operation conditions were appropriately selected, the high-order phase-locked vector soliton operation was always obtained in the laser. Experimentally, multiple such vector solitons with identical soliton parameters were also obtained. By carefully changing the pump strength, one could even control the number of vector solitons in a cavity, without changing the structure of the vector solitons. Like the scalar solitons observed in conventional soliton fiber lasers, harmonic mode locking of the high-order phase-locked vector solitons was also observed, as shown in Fig. 3, where 8 such vector solitons were equally spaced in the cavity. All of our experimental

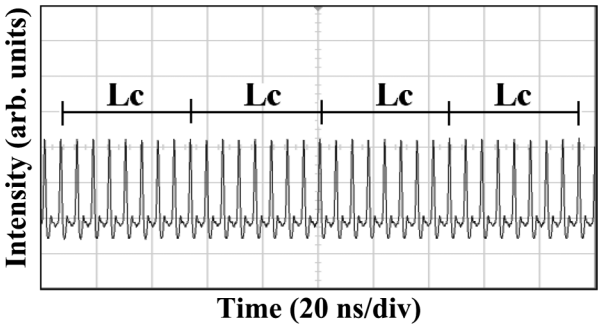

FIG. 3. Oscilloscope trace of a harmonically mode-locked high-order phase-locked vector soliton state. Lc: Cavity round-trip time. Eight vector solitons coexist in the cavity.

results show that the formation of high-order phase-locked vector solitons is a natural consequence of pulse circulation in the fiber laser under the current operation conditions.

To confirm our experimental observations, we also numerically simulated the operation of the laser. We used the following coupled Ginzburg-Landau equations to describe the pulse propagation in the weakly birefringent fibers in the cavity:

$$\frac{\partial u}{\partial z} = i\beta u - \delta\frac{\partial u}{\partial t} - \frac{ik''}{2}\frac{\partial^2 u}{\partial t^2} + \frac{ik'''}{6}\frac{\partial^3 u}{\partial t^3} + i\gamma\left(|u|^2 + \frac{2}{3}|v|^2\right)u + \frac{i\gamma}{3}v^2u^* + \frac{g}{2}u + \frac{g}{2\Omega_g^2}\frac{\partial^2 u}{\partial t^2},$$
$$\frac{\partial v}{\partial z} = -i\beta v + \delta\frac{\partial v}{\partial t} - \frac{ik''}{2}\frac{\partial^2 v}{\partial t^2} + \frac{ik'''}{6}\frac{\partial^3 v}{\partial t^3} + i\gamma\left(|v|^2 + \frac{2}{3}|u|^2\right)v + \frac{i\gamma}{3}u^2v^* + \frac{g}{2}v + \frac{g}{2\Omega_g^2}\frac{\partial^2 u}{\partial t^2}, \quad (1)$$

where u and v are the normalized envelopes of the optical pulses in the two orthogonal polarized modes of the optical fiber. $2\beta = 2\pi\Delta n/\lambda$ is the wave-number difference between the two modes. $2\delta = 2\beta\lambda/2\pi c$ is the inverse group velocity difference. k'' is the second-order dispersion coefficient; k''' is the third-order dispersion coefficient and represents the nonlinearity of the fiber. g is the saturable gain coefficient of the fiber, and Ω_g is the bandwidth of the laser gain. For undoped fibers, $g = 0$; for erbium-doped fiber, we considered its gain saturation as

$$g = G\exp\left[-\frac{\int(|u|^2 + |v|^2)dt}{P_{\text{sat}}}\right], \quad (2)$$

where G is the small signal gain coefficient and P_{sat} is the normalized saturation energy.

The saturable absorption of the SESAM is described by the rate equation:

$$\frac{\partial l_s}{\partial t} = -\frac{l_s - l_0}{T_{\text{rec}}} - \frac{|u|^2 + |v|^2}{E_{\text{sat}}}l_s, \quad (3)$$

where T_{rec} is the absorption recovery time, l_0 is the initial absorption of the absorber, and E_{sat} is the absorber saturation energy. We used the following parameters for our simulations for possibly matching the experimental conditions: $\gamma = 3\ \text{W}^{-1}\,\text{km}^{-1}$, $\Omega_g = 24$ nm, $P_{\text{sat}} = 50$ pJ, $k''_{\text{SMF}} = -23\ \text{ps}^2/\text{km}$, $k''_{\text{EDF}} = -13\ \text{ps}^2/\text{km}$, $k''' = -0.13\ \text{ps}^3/\text{km}$, $E_{\text{sat}} = 10$ pJ, $l_0 = 0.3$, $T_{\text{rec}} = 2$ ps, and cavity length $L = 10$ m.

We used the standard split-step Fourier technique to solve the equations and a so-called pulse tracing method to model the effects of laser oscillation [16]. We have always started our simulations with an arbitrary weak light input. Figure 4 shows one of the typical results obtained. With a cavity linear birefringence of $L_b = 3L$, a stable high-order phase-locked vector soliton state was obtained. The weak polarization component of the vector soliton consists of two bound solitons with pulse separation of $\sim$1 ps, while the strong polarization component of the

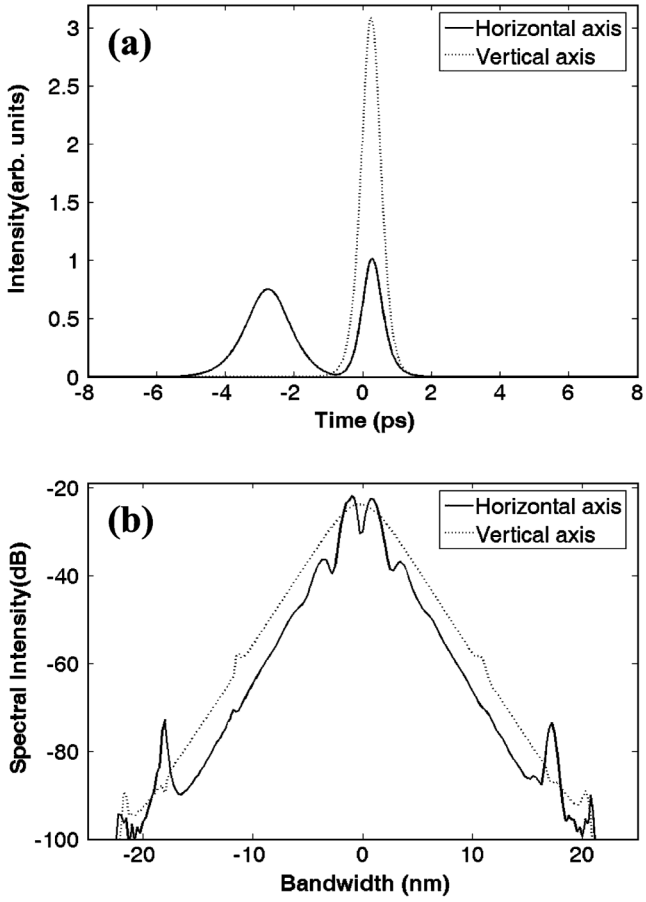

FIG. 4. A stable high-order phase-locked vector soliton state numerically calculated. (a) Soliton intensity profiles of the two orthogonally polarized components. (b) The corresponding optical spectra of (a).

vector soliton is a single-hump soliton. It is interesting to see that the pulse of the strong component is only temporally overlapped with one of the two pulses of the weak component. Because of the strong cross-phase coupling between the temporally overlapped pulses, the two pulses of the weak components have different pulse widths and intensities. Propagating within the cavity, obvious coherent energy exchange between the two temporally overlapped solitons is visible. Figure 4(b) further gives the calculated spectra of the vector soliton components, which also show that the phase difference between the two bound solitons of the weak component is 180°.

Depending on the laser parameters selected, other high-order phase-locked vector solitons, such as the one with both soliton components having a double-humped structure, were also numerically obtained. We note that similar high-order vector solitons were also predicted for pulse propagation in weakly birefringent fibers, but they are unstable. However, we found that all of the high-order phase-locked vector solitons obtained numerically were stable in the laser. We believe that the differences in stability of the high-order phase-locked vector solitons between fiber and fiber lasers could be traced back to their different soliton natures. While the soliton formed in a SMF is essentially a Hamiltonian soliton, the one formed in a fiber laser is a dissipative soliton, which is in fact a strange attractor of the laser system. The formation of multiple identical high-order vector solitons in the fiber laser clearly shows the dissipative nature of the vector solitons formed.

In conclusion, we have reported the first experimental observation of a type of high-order phase-locked vector soliton in a passively mode-locked fiber laser. The high-order vector soliton is characterized by the fact that its two orthogonal polarization components are phase-locked, and, while the stronger polarization component is a single-hump pulse, the weaker component has a double-humped structure with 180° phase difference between the humps. Our experimental results are the first confirmation of the theoretical predictions of high-order phase-locked vector solitons in birefringent dispersive media. Finally we note that, although the current experiment was conducted on a mode-locked fiber laser whose dynamics is governed by the coupled GL equations, due to the wide applicability of the coupled GL equations in describing the dynamics of real physical systems, it is expected that similar results could also be observed in other systems.

[1] L. A. Dickey, *Soliton Equations and Hamiltonian Systems* (World Scientific, New York, 2003).
[2] Y. S. Kivshar and G. P. Agrawal, *Optical Solitons: From Fibers to Photonic Crystals* (Academic, San Diego, 2003).
[3] L. F. Mollenauer, R. H. Stolen, and J. P. Gordon, Phys. Rev. Lett. **45**, 1095 (1980).
[4] C. R. Menyuk, Opt. Lett. **12**, 614 (1987); J. Opt. Soc. Am. B **5**, 392 (1988).
[5] M. N. Islam *et al.*, Opt. Lett. **14**, 1011 (1989).
[6] V. V. Afanasjev, Opt. Lett. **20**, 270 (1995).
[7] K. J. Blow, N. J. Doran, and D. Wood, Opt. Lett. **12**, 202 (1987).
[8] D. N. Christodoulides and R. I. Joseph, Opt. Lett. **13**, 53 (1988).
[9] N. Akhmediev, A. Buryak, and J. M. Soto-Crespo, Opt. Commun. **112**, 278 (1994).
[10] N. N. Akhmediev, A. V. Buryak, and J. M. Soto-Crespo, and D. R. Andersen, J. Opt. Soc. Am. B **12**, 434 (1995).
[11] N. N. Akhmediev, J. M. Soto-Crespo, S. T. Cundiff, B. C. Collings, and W. H. Knox, Opt. Lett. **23**, 852 (1998).
[12] S. T. Cundiff, B. C. Collings, N. N. Akhmediev, J. M. Soto-Crespo, K. Bergman, and W. H. Knox, Phys. Rev. Lett. **82**, 3988 (1999).
[13] B. C. Collings, S. T. Cundiff, N. N. Akhmediev, J. M. Soto-Crespo, K. Bergman, and W. H. Knox, J. Opt. Soc. Am. B **17**, 354 (2000).
[14] S. T. Cundiff, B. C. Collings, and W. H. Knox, Opt. Express **1**, 12 (1997).
[15] H. Zhang, D. Y. Tang, L. M. Zhao, and N. Xiang, Opt. Express **16**, 12 618 (2008).
[16] D. Y. Tang, L. M. Zhao, B. Zhao, and A. Q. Liu, Phys. Rev. A **72**, 043816 (2005).